I give permission for public access to my thesis and for copying to be done at the discretion of the archives' librarian and/or the College library.

_____ _____

Signature Date

Evidence of Hysteresis in the Neuromuscular System of 3rd Instar *Sarcophaga bullata*

By

Bethany A. Paterson

A Paper Presented to the

Faculty of Mount Holyoke College in

Partial Fulfillment of the Requirements for

the Degree of Bachelors of Arts with

Honor

Department of Biological Sciences

South Hadley, MA 01075

May, 2008

This paper was prepared
under the direction of
Professor Jacob Krans
for eight credits.

To SGM:
May I forever make you proud.

ACKNOWLEDGMENTS

I thank Professor Jake Krans for always believing in me, supporting me, and encouraging me throughout this research project. His patience with me, especially during the writing process, will forever be appreciated.

A special thanks to Hilary Selden for keeping me sane at all hours of the day.

Thank you Nancy Lech for all you help with ordering larvae and putting up with that awful stench across the hall.

The Mount Holyoke College Biology Department for providing funding for this project.

Curtis Smith for funding.

A special thanks to my family and friends for all the support and encouragement.

TABLE OF CONTENTS

LIST OF FIGURES

ABSTRACT

Hysteresis in neuromuscular systems is a marked deviation in force production from the predicted magnitude based on motoneuron rate. Third instar *Sarcophaga bullata* larvae were selected as model organisms for the investigation of hysteresis. Motoneurons exciting the longitudinal muscles of the larvae were stimulated using two different stimulus paradigms: (1) a constant stimulus frequency train, or '*tetanic*' and (2) a high frequency burst embedded within an otherwise constant frequency stimulus train, or *'hysteretic'*. The resulting isometric force production and intracellular muscle voltage were recorded.

Force production following the hysteretic burst(s) produced larger peak force than that predicted by tetanic stimulus alone. The largest changes in peak force occurred at the lowest tetanic stimulus frequencies. Tetanic and hysteretic stimuli paradigms yielded statistically indistinguishable forces by 20 Hz. The increased force production was not accounted for by the occurrence of synaptic facilitation during, or after, the high frequency burst as EJPs before and after hysteretic bursts were statistically indistinguishable. Taken together, these findings provide evidence for the action of hysteresis in third instar *Sarcophaga*.

Such findings suggest hysteresis could be a property mediated by the post-synaptic cell: the muscle itself. In an attempt to isolate the contribution of different contractile proteins to the hysteretic phenomenon, a high frequency burst was given at t = 1.5 s, during maximal contraction cycling of actin and myosin. These trials were compared to those with a high frequency burst at t = 2.5 s. The later onset time (t = 2.5 s) was chosen as a time at which myosin and actin cycling was approaching a constant cycle rate. There was no statistical different between force production from the varied onset stimulus time paradigms. Moreover, multiple burst stimuli resulted in uneven increases in force production with no muscle length change. Collectively, these results suggested hysteretic forces were not dependent upon the amount of overlap between actin and myosin.

INTRODUCTION

The functional units of skeletal muscles are the muscle fibers, or long cylindrical multinucleated cells (Berchtold et al., 2000). Muscle fibers are specialized cells that can develop tension, shorten, produce movement, and accomplish work (Sherwood, 2007). In mammals, a single neuron can innervate from one to over 25,000 muscle fibers (Purves et. al., 2004), and is called a motoneuron (MN). Thus, the control of muscle force production by the nervous system, particularly the MNs, is complicated. This makes a quantitative analysis of cause and effect in a mammalian neuromuscular system somewhat more involved than in simpler organisms.

Generally speaking, multiple steps must occur in the signaling cascade linking a MN signal to the end production of force. The synapse, or junction, of a MNs axon terminal with a muscle fiber occurs at what is called the neuromuscular junction (NMJ). Signals are initiated in the motoneuron as electrical charges (Figure 1A), or action potentials (APs; Figure 1B), which travel rapidly down the neuronal axon. Upon the arrival of an AP at the NMJ, a biochemical cascade results in the release of a signaling molecule that will cross the NMJ, known as a neurotransmitter (Usherwood, 1968; Onodera and Takeuchi, 1981). These chemical signals, upon reaching the muscle, elicit electrical potentials (Figure 1C) across the muscle cell membrane, which are known as electrical junction potentials (EJPs: Figure 1D). EJPs are the final electrical step in transducing the

nervous system's signal for muscle contraction (Purves et. al, 2004). Although the relationship between EJP and force is putatively a simple one (see below; Atwood 1967) much remains to be learned about the translation of a neuron's electrical signal to a muscle's physical output.

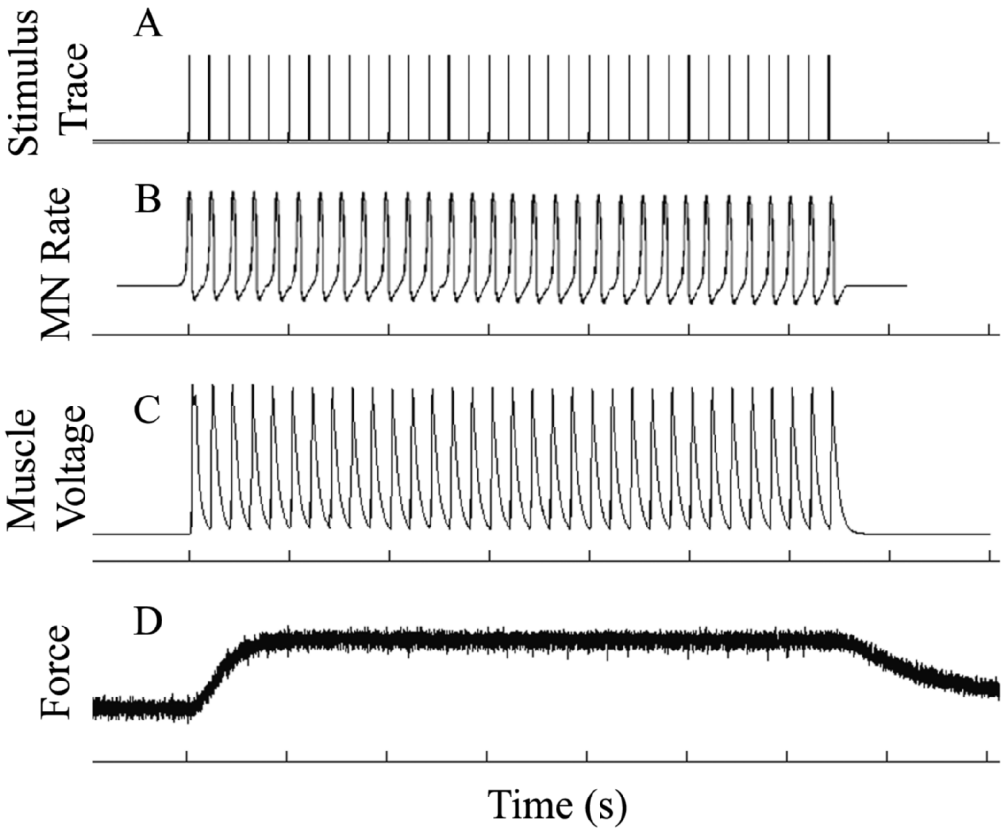

Figure 1. Neuromuscular transduction. (A) Constant stimulus frequency of the motor nerve at 5 Hz. (B) Resultant motoneuron (MN) action potential rate (schematic not to scale). (C) Electrical junction potentials (EJPs) across the membrane of the muscle cell. (D) Force generated by contracting muscle fibers.

To further complicate the understanding of general strategies in the control of force production, muscles can further be separated into several anatomically and physiologically disparate categories. Generally speaking, striated muscle cells make up skeletal and cardiac muscles of vertebrates, whereas smooth muscle

cells (unstriated) are often found in visceral and constitutively active applications such as the gastrointestinal system of humans. The striped appearance of striated muscle cells is an indication of a highly organized internal arrangement of muscle fibers (Figure 2A), each consisting of alternating, overlapping stacks of thick (myosin) and thin (actin) protein filaments in structural arrangements called sarcomeres (Sherwood, 2007). EJPs result from an influx of cations which increases the transmembrane potential of the cell, depolarizing the cell. The depolarization of the muscle cell by an EJP triggers the release of Ca++ ions from the sarcoplasmic reticulum, which binds to troponin on actin filaments. This leads tropomyosin to be physically moved aside to uncover cross-bridge binding sites on actin (Hill, 1952; Huxley, 2000). Powered by ATP, myosin cross-bridges attach to actin and bend, pulling the filament towards the center of the sarcomere (Figure 2B) to shorten the muscle (Spudich, 2001).

The two primary types of contraction are isotonic and isometric. In an isotonic contraction, muscle tension remains constant as the muscle changes length. Muscles do not shorten in isometric contractions, so muscle tension develops at a constant muscle length. The extent of actin and myosin overlap influences the amount of tension produced by a muscle fiber, with the maximum tension being produced at an intermediate level of overlap. As a muscle contracts isotonically the force it produces forms an unequal distribution over decreasing fiber lengths, with the maximum force occurring at intermediate lengths. (Sherwood, 2007) For this reason, comparisons between isometrically

contracting muscles are more informative so the muscles examined herein are stretched to comparable lengths and secured for isometric contraction.

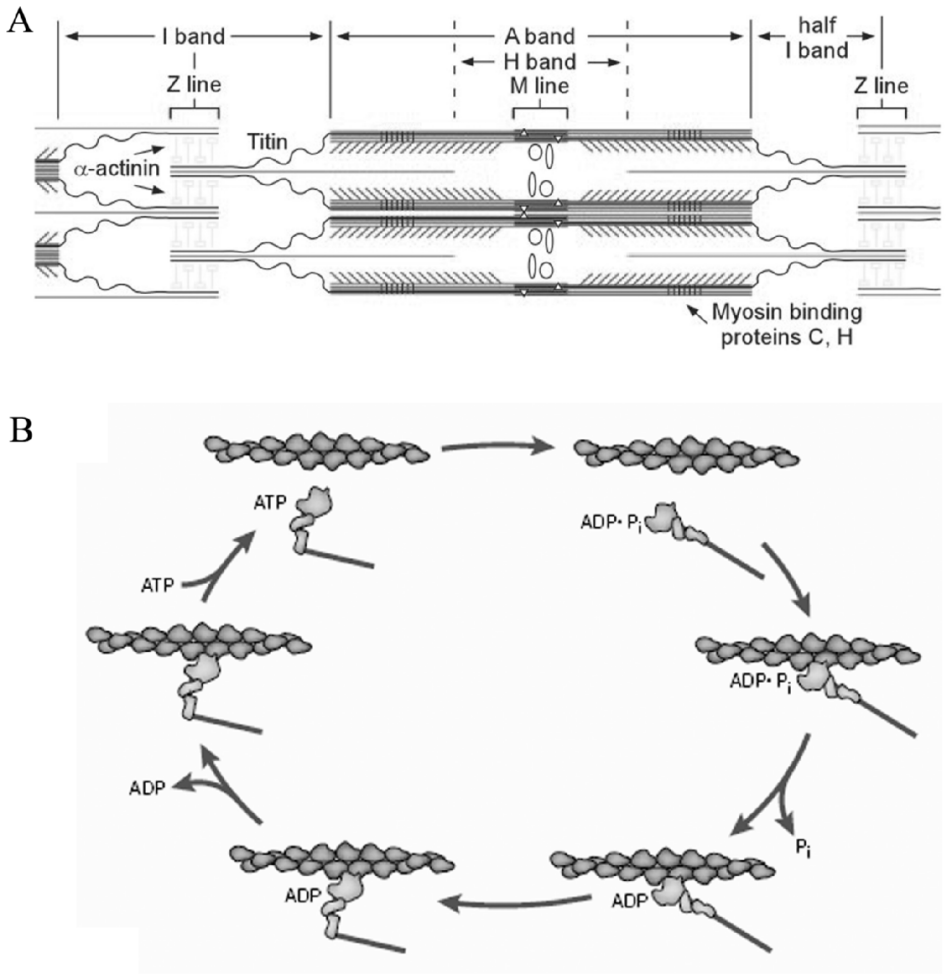

Figure 2. Invertebrate striated muscle sarcomere. (A) Arrangements of the thick (myosin) and thin (actin) filaments in the sarcomere (Hooper and Thuma, 2005). Titin and other integral proteins are shown. (B) The ATP powered cross-bridge cycling model of actin and myosin heads (Spudich, 2001). ATP is split by myosin ATPase and ADP+Pi remain on the myosin head during binding of actin. Phosphate is then released and energy stored in the cross-bridge powers the conformational change of the myosin head, pulling on the actin filament and contracting the sarcomere.

Responses of a muscle to stimuli can be categorized into two distinct types of contraction (Blaschko et. al., 1931). The response may be mediated by the physiological form of contraction: "slow-muscle" and "fast-muscle". Slow-muscle fibers can maintain tone for long periods of time, thus producing a continuum of force. Such characteristics make it useful in maintaining continuous behaviors, for example the utilization of slow contracting striated muscle by third instar larval *Diptera* during locomotion (Berrigan and Pepin, 1994). Fast-muscle (or fast-twitch muscle) shortens for comparatively quick, transient force generation – behaving like a switch that can turn force on and off. An extreme example of such contractions can be found in the asynchronous flight muscles of adult *Diptera*. Here, a single action potential triggers a series of contraction-relaxation cycles (Bullard, et al., 2006). A more familiar example is demonstrated in the arm muscles of humans, which are fast-twitch muscles used to perform transient movements such as lifting objects.

The storage of elastic strain energy is thought to be influenced by several structures and mechanisms, including the actin and myosin cross-bridges (Bennet-Clark, 1977) which account for a small amount of elasticity. More recently, it has been shown that elastic energy storage is largely determined by the giant protein titin (Tshhovrebova and Trinick, 2002). In vertebrates, titin molecules span half the sarcomere (Figure 2B) and provide flexible connections between the thick filaments and the Z-line of the sarcomere (Sherwood, 2007).

Studies discussed herein investigate non-linearities of the electrical portions of neuromuscular transduction. Dogma suggests the influence of MN AP rate on the muscle response is typically as follows: as the rate of motoneuron APs increases, so does the magnitude of force produced by the muscle. While a single AP can produce a single muscle twitch in some fibers, multiple twitches occurring in short succession result in twitch summation (Sherwood, 2007). The rapid increase in AP rate eliminates the relaxation phase and results in tetanus – a maximal sustained contraction (Figure 1D). Such a relationship suggests that a single force can be predicted from just one motoneuron rate, and the relationship is thus typically described as monotonic. However, early examples of nonlinearity in force generation (Blaschko et al., 1931), residual force enhancement in the isometric stretching of skeletal muscle (Abbott, 1952), or catch tension in arthropod muscle (Wilson and Larimer, 1968) illustrate a more complicated relationship between motoneuron rate and overall force production than those predicted by singular, monotonic, rate-force functions.

One explanation to account for the paradoxical relationship described above could be synaptic plasticity at the neuromuscular junction (Figure 3). Certain forms of plasticity – facilitation, augmentation, and post-tetanic potentiation – are relatively well understood means of modulation in the neuromuscular system (Zucker and Regehr, 2002; Stein, 2006). Other forms of nonlinearity in force generation, such as history dependent *post-synaptic* changes – generally referred to as hysteresis, remain poorly understood.

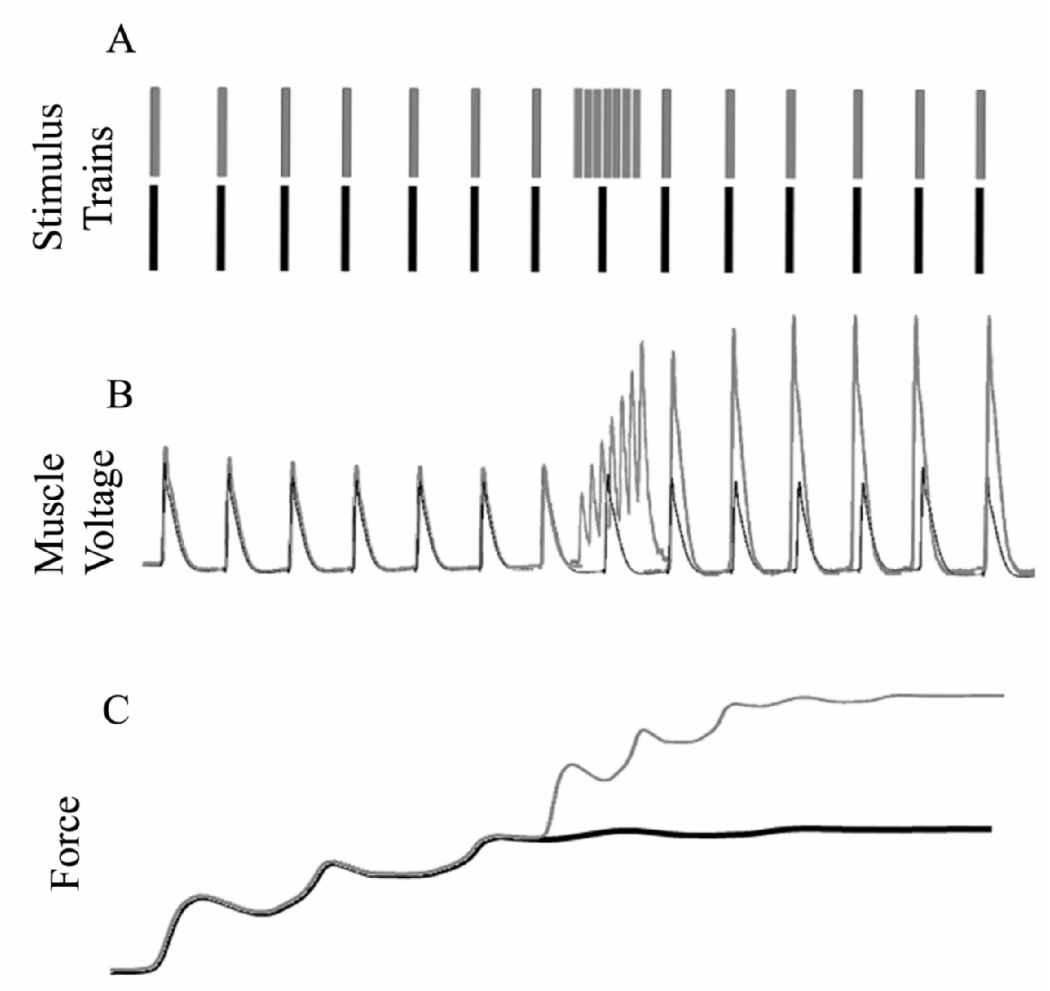

Figure 3. Illustration of synaptic facilitation at the neuromuscular junction. (A) Identical stimulus rates, but one also containing a brief, high frequency burst (***gray***). (B) Synaptic facilitation during and after the high frequency burst. (C) Non-linearity in overall force production. The consistent portion of MN rate across the two paradigms (***black***: tetanic, and ***gray***: tetanic + hysteretic burst stimulation protocol; see text) produces two different forces.

Hysteresis is an expression borrowed from the study of materials science (Song and Kiureghian, 2006). In the neuromuscular system, it manifests as a marked deviation in force production from the predicted magnitude based on motoneuron rate (Figure 4C). Assuming a constant MN rate produces a predictable peak force; force production would rise as a result of a high frequency burst, and then fall until it is maintained at the predicted force as indicated by the constant MN rate (Figure 4D); following rate as a simple dependent function. However, hysteresis is the failure of force to return to its predicted value. Upon termination of the hysteretic burst of APs (Figure 4A), force production falls initially but is maintained at a higher value than that predicted by the tetanic rate at which the muscle is being stimulated throughout the trial (Figure 4D). Thus, the output force can only be predicted by looking at *both* the immediately recent MN input *and* less recent, possibly transient history of MN rate. This phenomenon yields a unique nonlinear relationship in which one MN rate can produce multiple forces in muscle (Figure 4D).

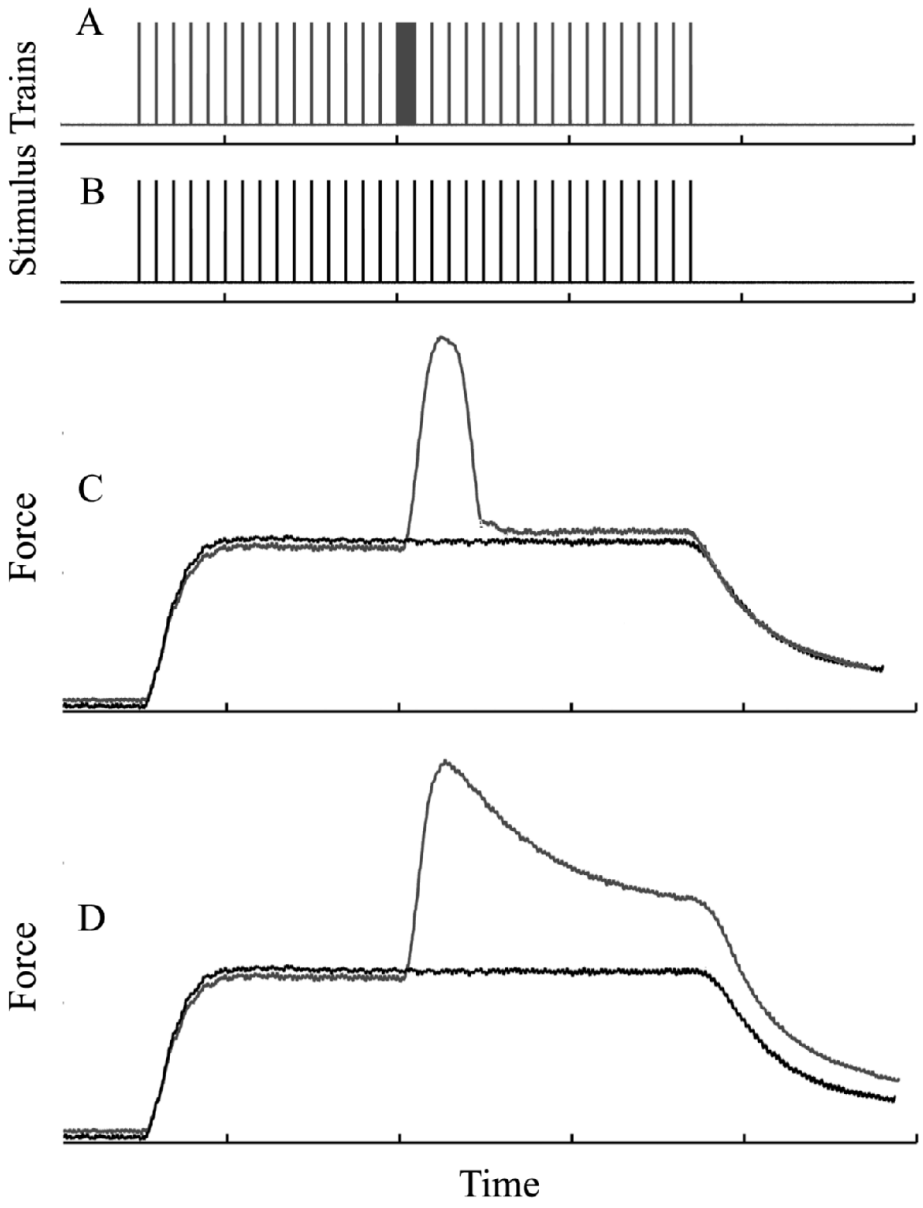

Figure 4. Schematic of predicted force production and hysteresis. (A) Tetanic stimulus train with hysteretic burst. (B) Constant frequency, tetanic stimulus trace. (C) Predicted force relationship as indicated by a simple monotonic relationship between MN rate and force production. Force rises as a result of the high frequency burst and return to the predicted value after the high frequency burst. (D) Hysteretic force relationship in which force rises transiently as a result of the high frequency burst but then *remains* elevated, failing to return to the predicted value.

Nonlinearities of force production during cyclical or long-duration contractions have been investigated in a number of vertebrate and invertebrate muscles through characterization of the muscle's work loop (Wilson and Larimer, 1968; Wilson, Smith, Dempster, 1970; Bennet-Clark, 1977; Josephson and Stokes, 1989; Josephson and Stokes, 1993). A work loop records force production as the motoneuron is stimulated with a steadily modulated frequency that continuously increases or decreases in rate (Figure 5D). The motoneuron is gradually stimulated to the point of force saturation and then the stimulus rate is reduced (Figure 5C). Work loops thus show the history dependent characteristics (hysteresis) of the muscle, as muscle force fails to return to its original value. The elevated upper portion of the work loop indicates a maintained increase of force production after recent exposure to an accelerated AP rate. A system with no hysteresis would be characterized by a single line, (monotonic) irrespective of recent history, rather than a loop-shaped plot.

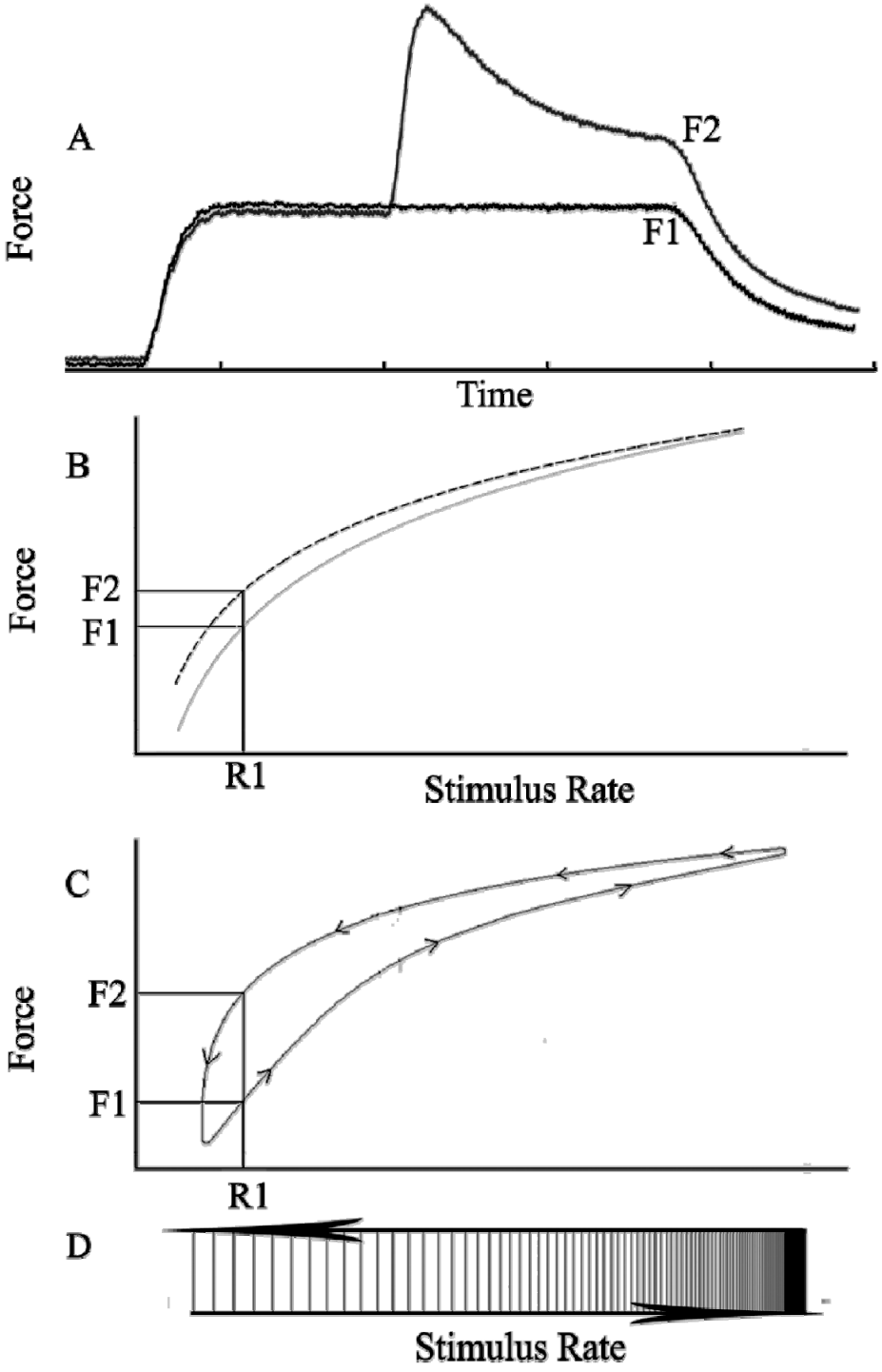
A
Force
F2
F1
Time
B
Force
F2
F1
R1
Stimulus Rate
C
Force
F2
F1
R1
D
Stimulus Rate

Figure 5: Hysteretic work loop. (A) Force production illustrating two different forces (F1 and F2) at a single MN rate. (B) Single motoneuron rates can produce two different forces over a continuum of MN rates. (C) Hysteretic force production shown as a work loop. The MN is gradually stimulated to the point of saturation (left to right, bottom) and then the stimulus rate is reduced (right to left, top) as illustrated in (D).

Experiments discussed herein investigate three related questions of history-dependent plasticity in a model organism: (1) Do the larval muscles of large flies (i.e. *Muscid, Calliphorid* or S*arcophagid*) exhibit plasticity in force production? (2) Is the muscle plasticity a hysteretic phenomenon, or is it simply a result of synaptic facilitation during the high frequency burst? (3) If hysteresis is not due to voltage, as would be the case with synaptic facilitation, what molecular mechanisms could account for it? The importance of elucidating the hysteretic behavior of muscle is relevant in two realms, previously outlined by Wilson, Dean, and Dempster (1970). (1) Hysteresis appears to be a general property of muscle. It has been reported in mammalian striated muscle (Partridge, 1966), insect and crustacean slow muscles (Wilson and Larimer, 1968), and frog striated muscle (Lappin et al., 2006). (2) The hysteretic phenomenon in force production indicates that there can be significant changes in the way that muscle translates motoneuron electrical potentials to resultant force.

In order to investigate hysteresis, we choose to work with third instar, wandering stage, *Sarcophaga bullata*. Arthropods make up over ¾ of all living and fossil organisms, with *Diptera* as one of the four largest orders among all living animals. The common ancestor of both invertebrates and vertebrates had muscle, and the relative simplicity of invertebrate preparations offers an

experimental advantage for the investigation of their shared proteins (Hooper and Thuma, 2004). More specifically, *Sarcophaga* are model organisms in that they are straightforward to rear, have a simple geometric and repetitive anatomical organization of their muscles and nerves, and are robust *in vitro*. Moreover, their large longitudinal muscles are innervated by relatively few motoneurons. During the wandering stage, the larvae cease feeding and search for suitable pupariation sites. To accomplish the locomotion necessary for that behavior, a small number of bodywall muscles undergo series of rhythmic, peristaltic contractions (Berrigan and Pepin, 1994).

I hypothesize that the neuromuscular systems of third instar S*arcophaga* larvae will exhibit hysteresis. Thus, the increased force will not be explained by synaptic facilitation during or after the high frequency, hysteretic, burst. Furthermore, I speculate that hysteresis is not due to changes at either the neuron or synaptic levels, but rather resides in changes to the contractile proteins, or proteins closely associated with contraction found in the muscle. To logically explore this hypothesis, I initially examined the roles of actin and myosin during different cycling periods, and what happened when the cycling was interrupted. The protocol for this experiment changed the onset of the high frequency burst to occur during the shortening phase of actin and myosin. Finally, I was curious to test the elastic properties of titin through stretching. Similar to the properties of an elastic rubber band, I expected to see a decrease in elasticity as the titin molecule continued to stretch by the multiple burst hysteretic stimuli.

MATERIALS AND METHODS

Animals & Preparations

Third instar, "wandering" stage, *Sarcophagidae bullata* were purchased from Carolina Biological Supply. Thereafter, they were reared in plastic containers containing a custom food recipe (adapted from Jeff Scott at Cornell University's Entomology Department, personal communication) which included pre-mixed larval medium (Carolina Biological Supply), raw beef liver, dried milk and sugar. Containers were maintained in a 20°C incubator on a 12-12 light-dark cycle until larvae tanned. Newly eclosed adult flies were moved to a new container with fresh food, scored beef liver, dried milk and sugar.

Two physiological preparations were used: (1) isometric force recordings and (2) intracellular voltage recordings. For each dissection, larvae were initially pinned at their posterior and anterior apexes to a Sylgard-lined dish (Dow Corning Corporation, Midland, MI), ventral surface down. Preparations were immersed in insect ringers (after Strausfeld, 1972) and a shallow longitudinal incision was made from posterior to anterior along the dorsal surface. The guts and tracheae were removed to expose the bodywall musculature, neuromuscular junction, and segmental nerves (Figure 6). The larva was firmly stretched, filleted with six insect pins (size 00; VWR International, West Chester, PA), and the segmental nerves were severed. Pins were placed between the cuticle and bodywall musculature and remained in place during voltage experiments. In force

experiments, dissecting pins were removed after positioning the stimulus electrode (described below).

Physiology

All electrophysiological experiments were performed in a Faraday cage under a dissecting microscope. Preparations were bathed in insect ringers and temperature was maintained between 16-18°C via recirculation of coolant through the preparation stage. Suction electrodes were used to stimulate segmental nerves in both force and voltage preparations. These were made with 1.0 mm IN thin wall glass microcapillary tubes containing filaments (World Precision Instruments, Inc., Sarasota, FL). Individual electrodes were pulled by a P-87 Flaming/Brown Micropipette Puller (Sutter Instrument Co., Novata, CA). Tips were broken off and fire-polished to the desired luminal opening for nerve suction.

Isometric forces were recorded using a custom strain gauge and simple tabs attached to either end of the larva. Two Plexiglas tabs, with attached metal hooks, were secured to the dissected larvae using cyanoacrylate (Figure 6). Once attached to the animal, one tab was firmly secured to the preparation dish by a large pin placed into the Sylgard . The other was attached to the beam of a custom built strain gauge force transducer consisting of four silicon wafers in a full Wheatstone Bridge circuit.

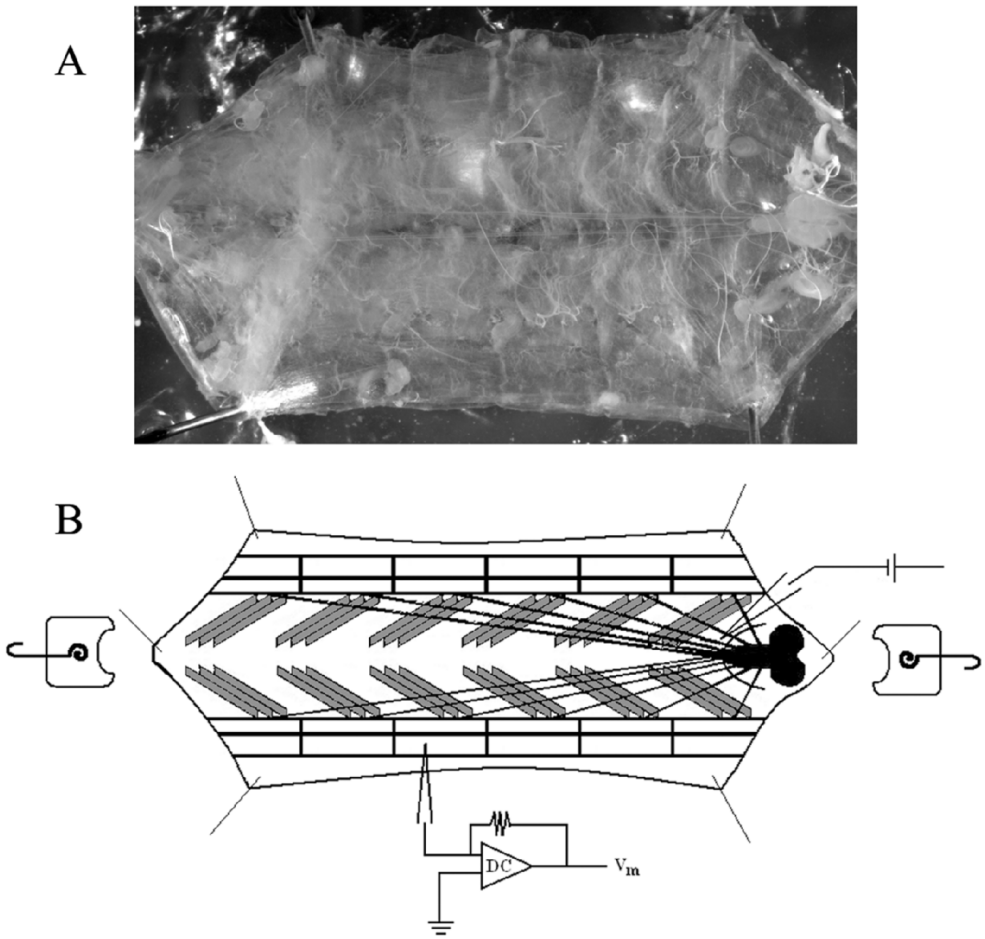

Figure 6: Larval *Sarcophagid* anatomy. (A) A filet-type dissection of the third instar, wandering larva. The single ventral ganglion is apparent on the far right as semi-spherical light objects in *A* (right = anterior) and black in *B*. Intact nerves are present along the central longitudinal axis and are flanked by the longitudinal muscles. (B) A schematic of the connections between segmental nerves and musculature is given for visualization only. The longitudinal muscles shown along the perimeter of the schematic were used in this study. Stimulating and recording electrodes are shown, and plastic tabs used for force measurement are shown on the far right and left.

Severed segmental nerves were gathered with a suction electrode and were stimulated via electrical current for both force and voltage recordings. Electrical current was modulated by a Grass S88 stimulator (Grass Instruments, West Warwick, RI) and traveled through a Grass SIU5 Stimulus Isolation Unit (Grass Instruments, West Warwick, RI). The isolation unit was set at 1.00 and 0.01 for force and voltage recordings, respectively. Stimulation of the segmental nerves evoked junction potentials and contractions, which were transformed to voltage by the force transducer. Trials were displayed on an oscilloscope (Tektronix, Beaverton, OR) and recorded using a National Instruments DAQ board and the MATLAB DAQ toolbox

Timing of stimulus trains were controlled using custom MATLAB routines (MathWorks, Natick, MA). Three different experimental stimulus paradigms were used: (A) tetanic, (B) hysteretic burst, and (C) multiple hysteretic bursts (Figure 7). Tetanic stimulation (A) involved a simple train of stimuli at a constant frequency (Figure 7A). Hysteretic stimulation (B) used the same constant rate as in the tetanic condition, and included a 200 ms high frequency burst occurring before the end of stimulation (Figure 7B). Onsets for the high frequency burst varied and included $t = 1.5$ s, $t = 2.5$ s, or $t = 4.0$ s. Multiple hysteretic stimulation (C) utilized a constant stimulus rate with the occurrence of three 200 ms high frequency bursts occurring at $t = 4.0$ s, $t = 7.0$ s, and $t = 10.0$ s (Figure 7C).

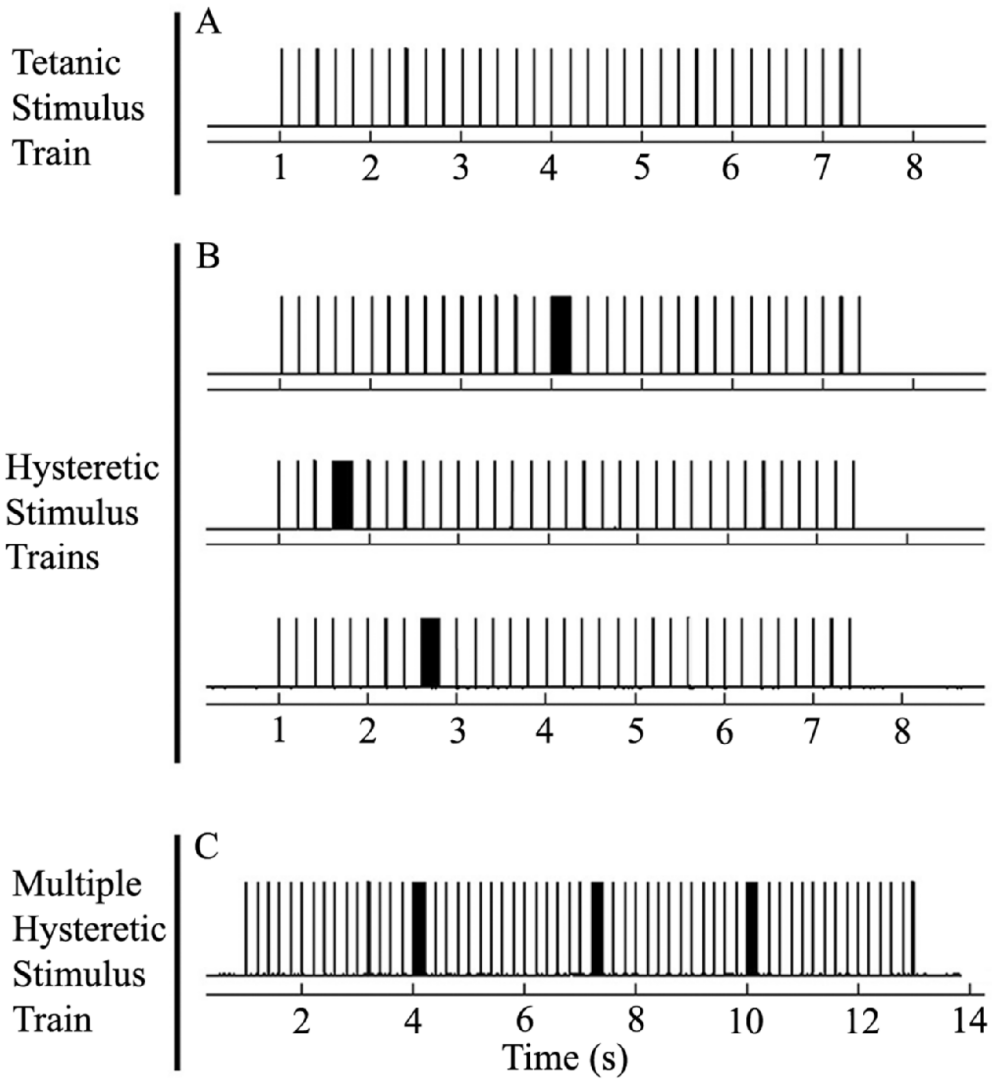

Figure 7: **Schematic of the experimental MN stimulus paradigms**. (A) Tetantic stimulus train at 5 Hz. (B) Hysteretic stimulus trains at 5 Hz with a 200 ms 50 Hz high frequency burst at varied onsets (t = 4.0 s, 1.5 s, and 2.5 s). (C) Multiple hysteretic stimulus train at (tetanic = 5 Hz) with a 200 ms 50 Hz hysteretic, high frequency burst occurring at t = 4.0, 7.0, and 10.0 s.

Larval length and stimulus threshold were modified for all animals before force recordings were initiated. Comparable points on the length tension curve of all animals were identified by manually stretching the longitudinal muscles. Single stimuli were applied after each lengthening to select for the peak force production. Lengthening stopped once the peak of the length-tension curve was identified. Stimulus threshold was then established using single stimuli to produce a short muscle contraction. The stimulus magnitude that yielded the greatest force production from the single twitch was noted for further stimulation. The final stimulus magnitude used for the experiments was set at approximately 125% of the identified threshold. Between10 to 20 repetitions of each stimulus paradigm, with intertrial pauses of 45 s (for tetanic), 65 s (for hysteretic), and 90 s (for multiple hysteretic bursts), were conducted for each stimulus rate.

During intracellular recordings, the longitudinal muscles were tightly stretched lengthwise, and the larva was completely submerged in insect ringers. A newly pulled microelectrode was filled with 2 M potassium acetate and was mounted to a micromanipulator (Narishige International USA, Inc., Long Island, NY). Electrode resistance varied between 10-60 MΩ. The intracellular electrode penetrated the longitudinal muscle as normal to the surface of the cell membrane as possible. EJPs within the muscle were measured via an AxoClamp-2A amplifier (Axon Instruments, Union City, CA). Between 5 to 20 repetitions of the hysteretic and tetanic stimulus paradigms, with intertrial pauses of 15s, were conducted per stimulus rate.

RESULTS

Tetanic stimulation of the motoneurons, described above, of 3rd instar *Sarcophaga* resulted in the temporal summation of force twitches and complete tetanus (Figure 8A). Tetanic stimulus trains lasted 3 s, from t ~1 s to t ~4 s. Force generation was calculated as the change from baseline, and was measured at t ~4 s. Final force values were normalized to the peak force observed from the animal stimulated at 50 Hz. Force generation increased with MN rate (stimulus rate) in a logarithmic fashion (Figure 8B). Force generation reached nearly 100% saturation using a 20 Hz stimulus rate (0.9158 (±0.0338)). The maximum force generation of 1.0650 (±0.0176) occurred using a stimulus rate of 40 Hz.

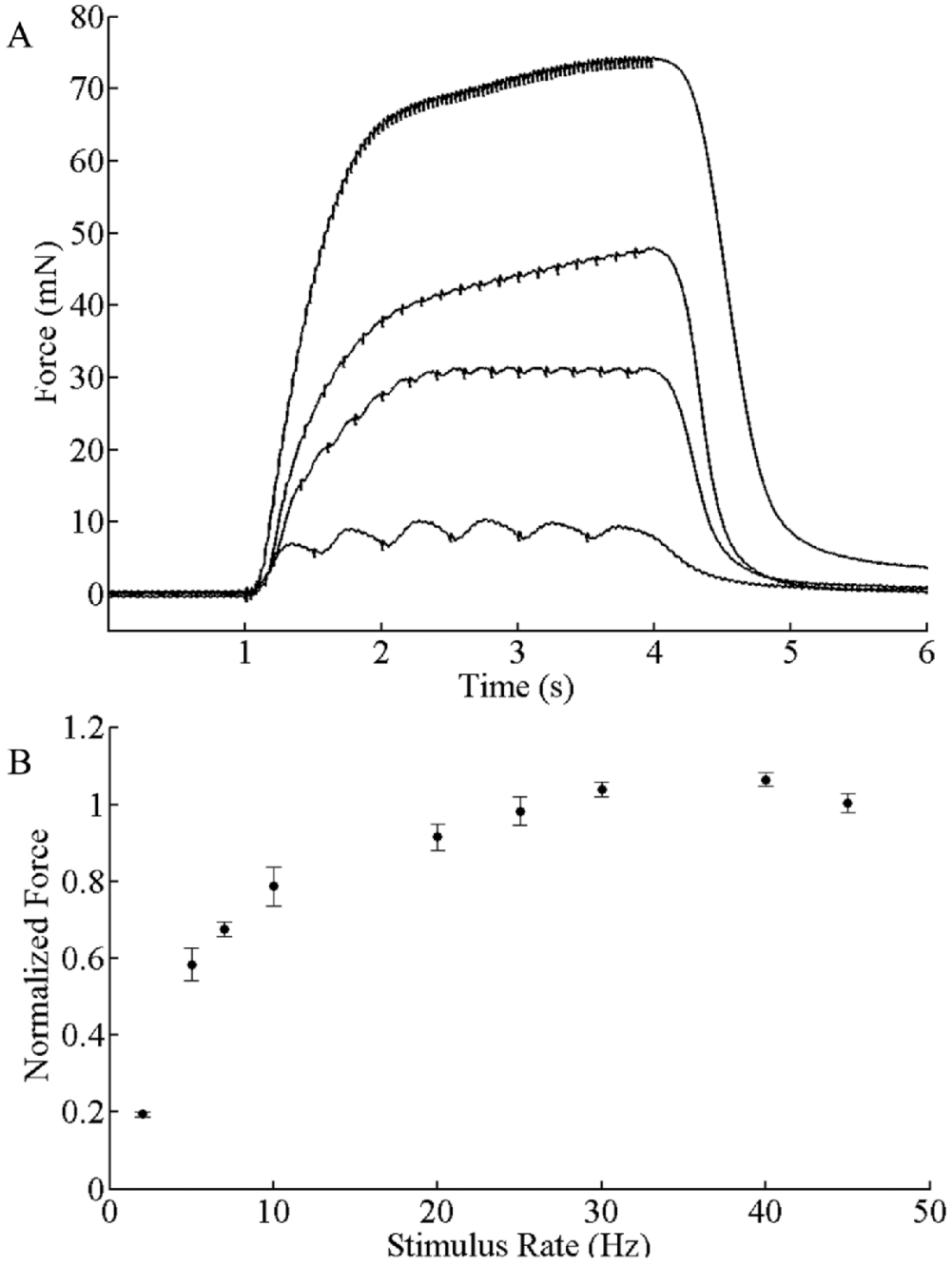

Figure 8: **Tetanic force production across multiple MN rates**. (A) Force recordings from a single *Sarcophaga* at 2, 5, 7, and 50 Hz. Traces in *A* are averaged from five trials and Butterworth filtered to reduce high frequency noise (≥ 5 KHz). (B) Values are normalized to the peak force observed from the animal stimulated at 50 Hz. Data points represent the average of 25 trials per stimulus rate with an average of 4 animals used per stimulus rate (total animals used (n) = 7), errorbars = standard error of the mean.

Tetanic stimulus paradigms were expanded from a 3 s stimulus time to a 6.5 s stimulus time. Hysteretic stimulus paradigms included a high frequency burst (50 Hz for 200 ms) occurring 3 s into the constant stimuli paradigm at t ~4 s. Force generation was measured as the change from baseline at t ~6.5 s, and was normalized to the peak force observed from the animal stimulated at 50 Hz. T-tests (assuming unequal variance) were used to compare mean force generation between tetanic and hysteretic stimulus paradigms.

At low MN rates, the addition of a high frequency burst yielded significantly higher force values than tetanic stimulus trains alone. Specifically, at a stimulus rate of 2 Hz, hysteretic burst paradigms gave statistically greater force than tetanic stimulation alone ($P < 0.01$) (Figure 9A). Similarly, at 5 Hz ($P = 0.058$) and 7 Hz ($P = 0.058$), hysteretic paradigms yielded statistically greater force than tetanic paradigms. Higher hysteretic forces were evident using rates of 10 Hz, 12 Hz, and 15 Hz, but these were not statistically different than force generated by equivalent tetanic rates. By 20 Hz, tetanic and hysteretic stimulus paradigms yielded nearly identical forces (Figure 9B). The nature of the relationship was particularly evident when the percent increase in force during hysteretic trials was plotted versus stimulus rate (Figure 9C). Hysteretic forces were 109.8% of tetanic forces (more than double) when muscles were stimulated at 2 Hz, and the increased force during hysteretic trials decreased progressively to 1.8% percent using a 20 Hz stimulus rate. These data were well fit by a logarithmic function (Figure 9C; Pitman's normal correlation, $P < 0.01$).

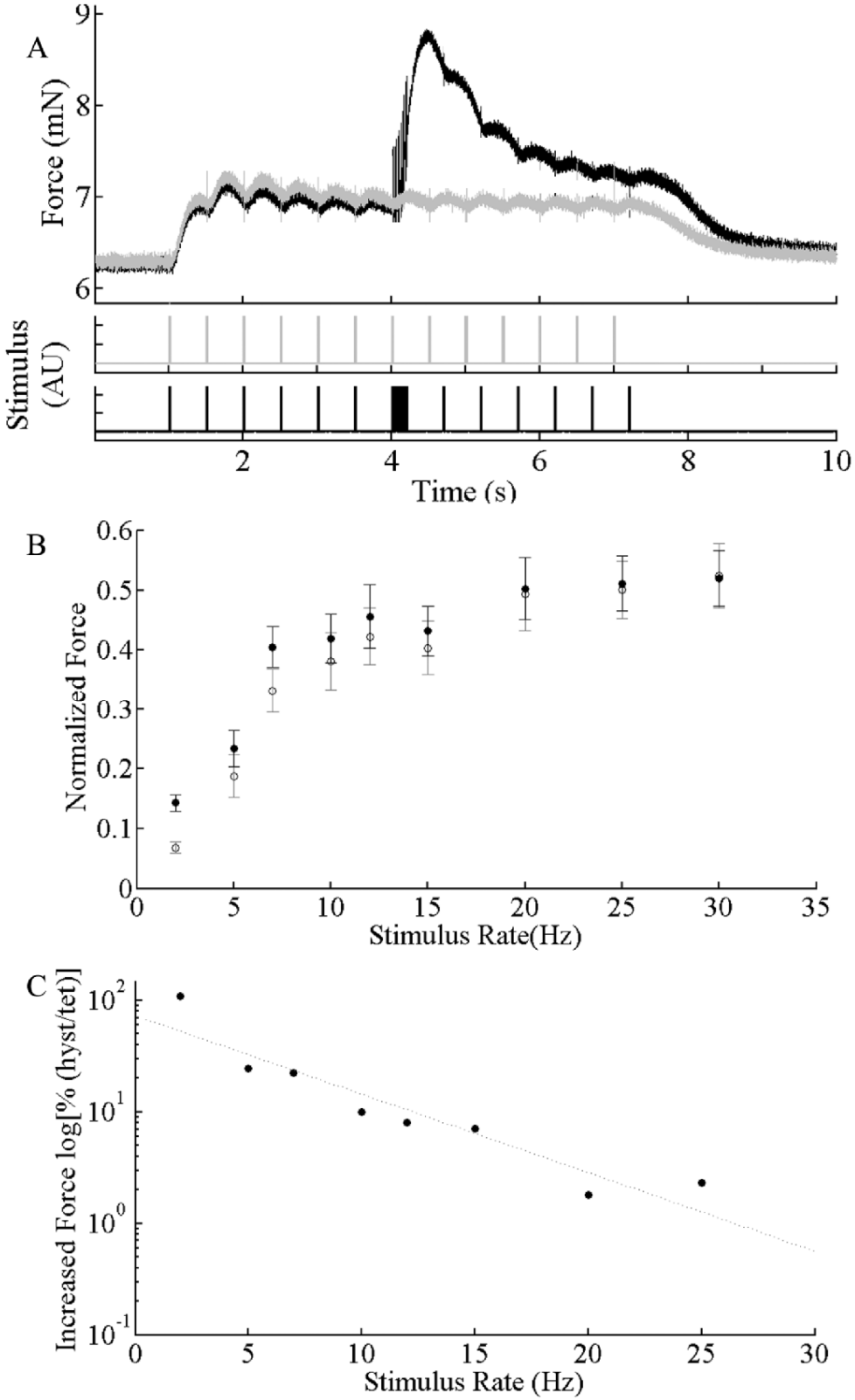
A
Force (mN)
9
8
7
6
Stimulus (AU)
2
4
6
8
10
Time (s)
B
Normalized Force
0.6
0.5
0.4
0.3
0.2
0.1
0
0
5
10
15
20
25
30
35
Stimulus Rate(Hz)
C
Increased Force log[% (hyst/tet)]
10^2
10^1
10^0
10^{-1}
0
5
10
15
20
25
30
Stimulus Rate (Hz)

Figure 9: **Force generation as a function of motoneuron rate in hysteretic versus tetanic stimulus paradigms.** (A) Each trace is the average of 5 repetitions in a single animal. Data from the tetanic paradigm are shown in black, whereas those recorded from a hysteretic paradigm (involving a 200 ms, 50 Hz burst at t ~4 s) are shown in gray. Force produced from the hysteretic trials exceeds that predicted by tetanic trials and is maintained for the duration of the trial(s). (B) Values are normalized to the peak force observed from the animal stimulated at 50 Hz. Data points represent the average of ten trials per animal, with 4-6 animals used per frequency (n = 30). Hysteretic force is significantly different at 2 Hz ($P << 0.01$). Both tetanic (◦) and hysteretic (•) forces saturate at relatively low stimulus frequencies. Standard error of the mean is shown. (C) The hysteretic burst produces larger relative changes in peak force at lower stimulus frequencies. This is shown as percentage change in peak force over a range of stimulus frequencies. A logarithmic equation (coefficients = -0.16 and 4.29) fits the data well (Pitman's normal correlation; $P < 0.01$).

Transmembrane voltage recordings utilizing the same hysteretic and tetanic stimulus paradigms revealed the increased force production was not accounted for by the occurrence of synaptic facilitation during the high frequency burst (Figure 10A). EJP amplitudes before and after the hysteretic burst were compared across stimulus frequencies (Figure 3B). Both sets of data are well fit by the same line (Figure 10B; Pitman's normal correlation; $P < 0.01$). This suggests that no observable amount of synaptic facilitation or potentiation occurred during the high frequency burst.

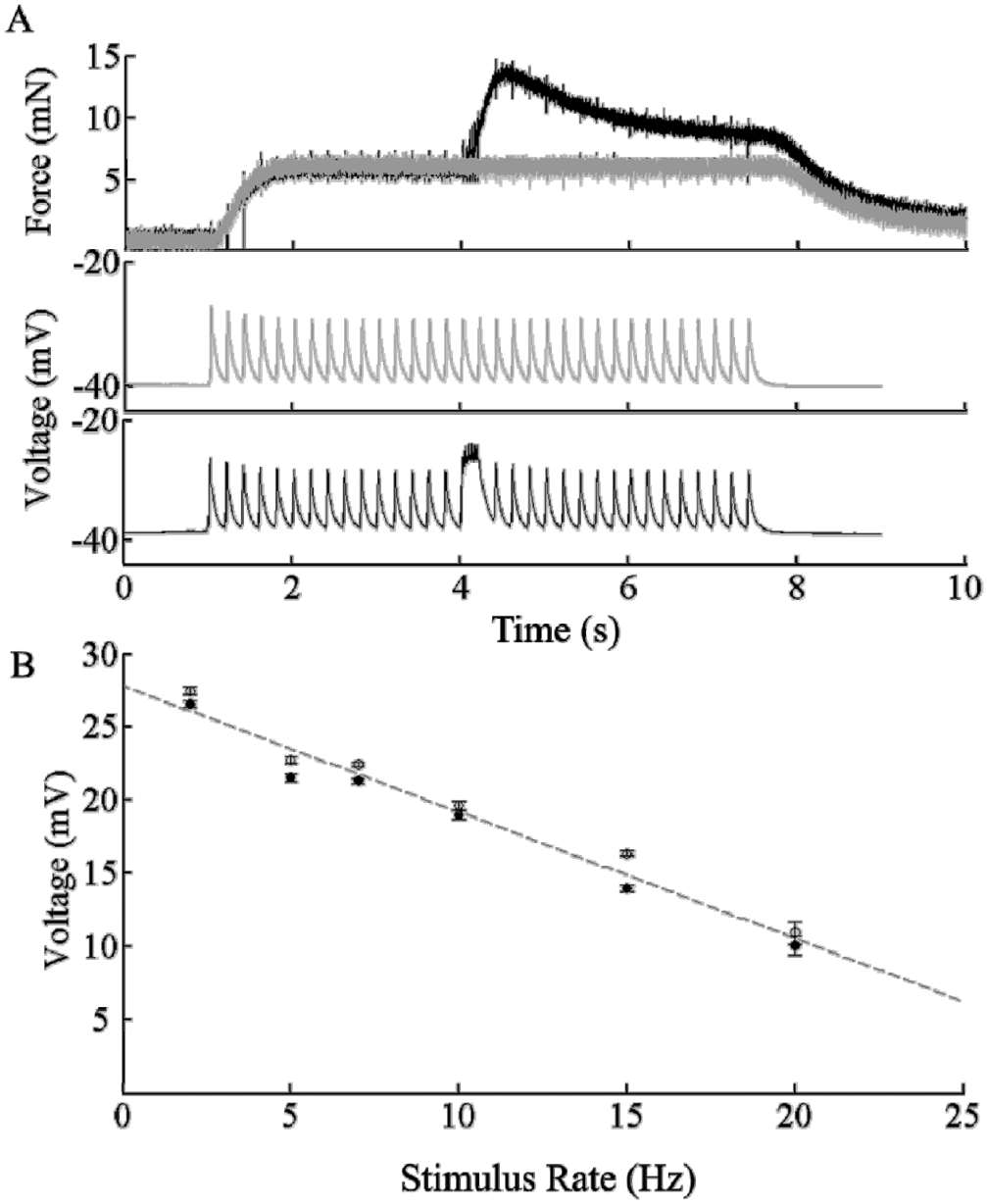

Figure 10: Agreement of EJP amplitude before and after a hysteretic burst. (A) EJP amplitude and force production. Each force trace is an average of five trials from a single animal at 5 Hz (no filtering). Representative voltage recordings of a single tetanic and a single hysteretic stimulus train taken from a different animal are shown below. (B) EJP amplitude was indistinguishable across rates. Data are well fit by the linear function V= -0.86(Rate) + 27.83 (R^2 = 0.97, $P < 0.01$).

EJP amplitude decreased as stimulus rate increased, revealing a negative correlation and suggesting the occurrence of synaptic depression at the neuromuscular junction during higher frequencies. EJPs recorded during tetanic paradigms were compared at stimulus rates of 2 to 20 Hz (Figure 11A). Membrane potential was maintained at -70.48 (±0.19) mV for the 2 Hz stimulus train and showed no signs of temporal summation or any gradual depolarization of baseline membrane potential. Similar findings were evident with the 20 Hz train, with the exception of an increase in membrane potential from -59.84 (±0.10) mV to -48.80 (±0.15) mV after the first second, where it was maintained (n = 4; Figure 11D). Maximum (peak) EJP voltage remained consistent across the duration of the 2 Hz tetanic stimulus train(s). Peak voltage occurred at t ~1 s and then decreased to -25.96 (±0.24) mV, where it was maintained for the duration of the trial (Figure 11C). No evidence of synaptic depression was evident in either stimulus train as maximum peak voltage does not decrease over time. Mean peak voltages across the 7 s trials were -49.84 (±1.24) mV and -25.48 (±2.20) mV for 2 Hz and 20 Hz, respectively (Figure 11C). The maximum EJP amplitude was calculated at t ~1 s, and measured 39.34 (±0.11) mV in the 20 Hz train (Figure 11B). EJP amplitude was there after maintained at a 22.88 (±0.33) mV. In the 2 Hz train, EJP amplitude gradually decreases over the first two seconds of the stimulus train and then was maintained at 20.08 (±0.14).

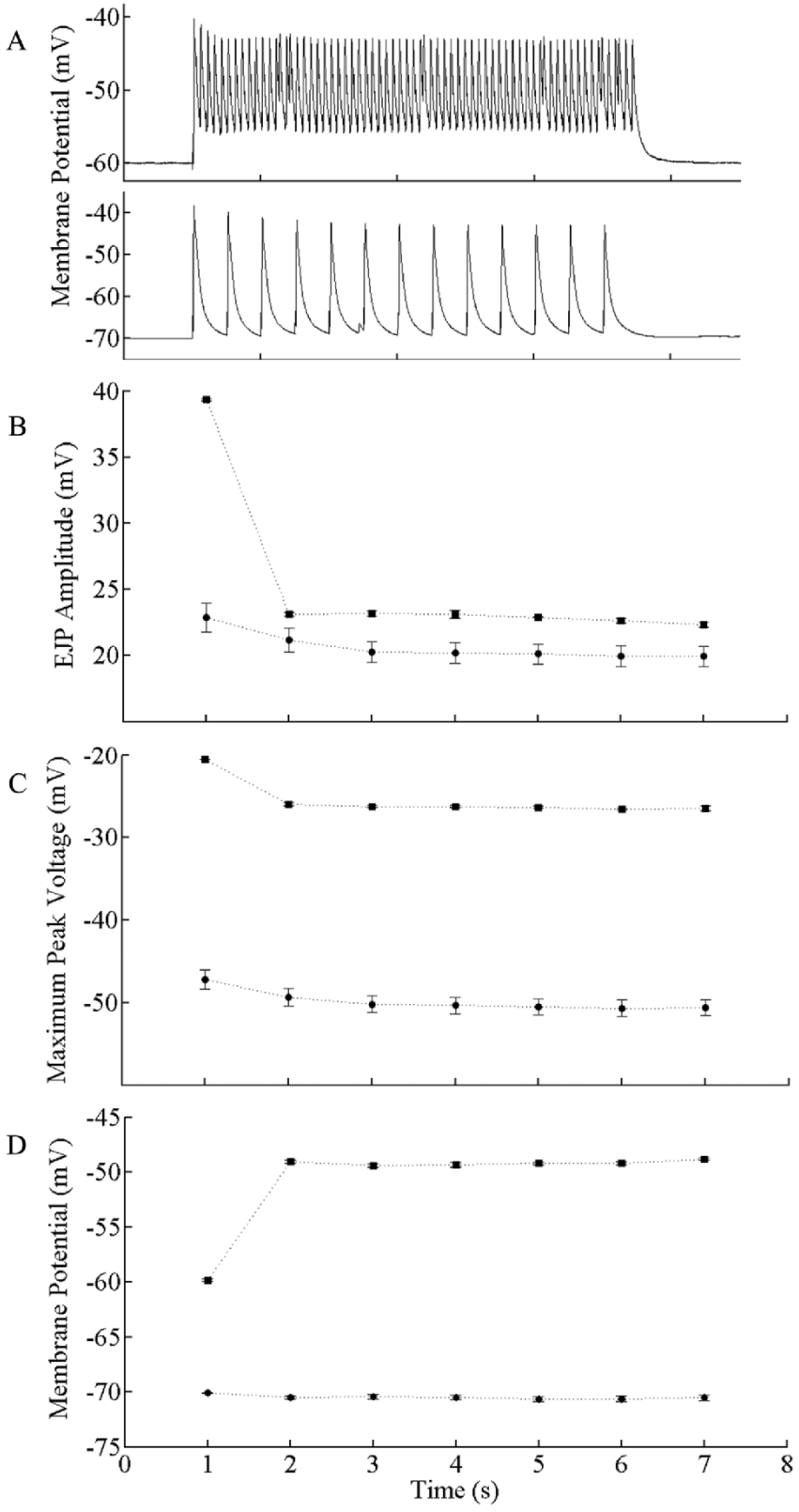
A
Membrane Potential (mV)
-40
-50
-60
-40
-50
-60
-70
B
EJP Amplitude (mV)
40
35
30
25
20
C
Maximum Peak Voltage (mV)
-20
-30
-40
-50
D
Membrane Potential (mV)
-45
-50
-55
-60
-65
-70
-75
0
1
2
3
4
5
6
7
8
Time (s)

Figure 11: Larval EJP properties and frequency dependent characteristics. (A) EJP voltage traces from a 20 Hz stimulus train and a 2 Hz stimulus train (n = 2 animals, 2 muscles). (B) Membrane potential remains consistent across the time duration of the trials for 2 Hz. Membrane potential decreases from t = 1 to 2 s and then is maintained at about -50 (± 4.03) mV for the 20 Hz stimulus. (C) Local maxima of the EJP (peak) remains at a relatively constant voltage for the duration of the trial when stimuli are delivered at 2 Hz. The local maximum occurred at t = 1 s and then decreased to ~-25 mV thereafter, where it remained for the duration of the trial. There is no evidence of synaptic depression. (D) EJP amplitude occurs at its maximum level at t = 1 s and is thereafter maintained at a consistent level in the 20 Hz train. EJP amplitude gradually decreases over the first two seconds of the stimulus train and then is maintained in the 2 Hz train.

In an attempt to isolate the contributions of different contractile proteins to the hysteretic phenomenon, the onset time of the high frequency burst was varied during hysteretic stimulus trains. A high frequency burst was given at t = 1.5 s, during maximal contraction cycling of actin and myosin (Figure 12A). These trials were compared to those with a high frequency burst at t = 2.5 s. The later onset time (t = 2.5 s) was chosen as a time at which myosin and actin cycling was approaching a constant cycle rate. Force generation was measured as the change from baseline at t ~6.5 s, and was normalized to the peak force observed from the animal stimulated at 50 Hz. T-tests (assuming unequal variance) were used to compare mean force generation between tetanic and hysteretic stimulus paradigms. There was no statistical different in force production between the varied onset stimulus time paradigms (Figure 12B).

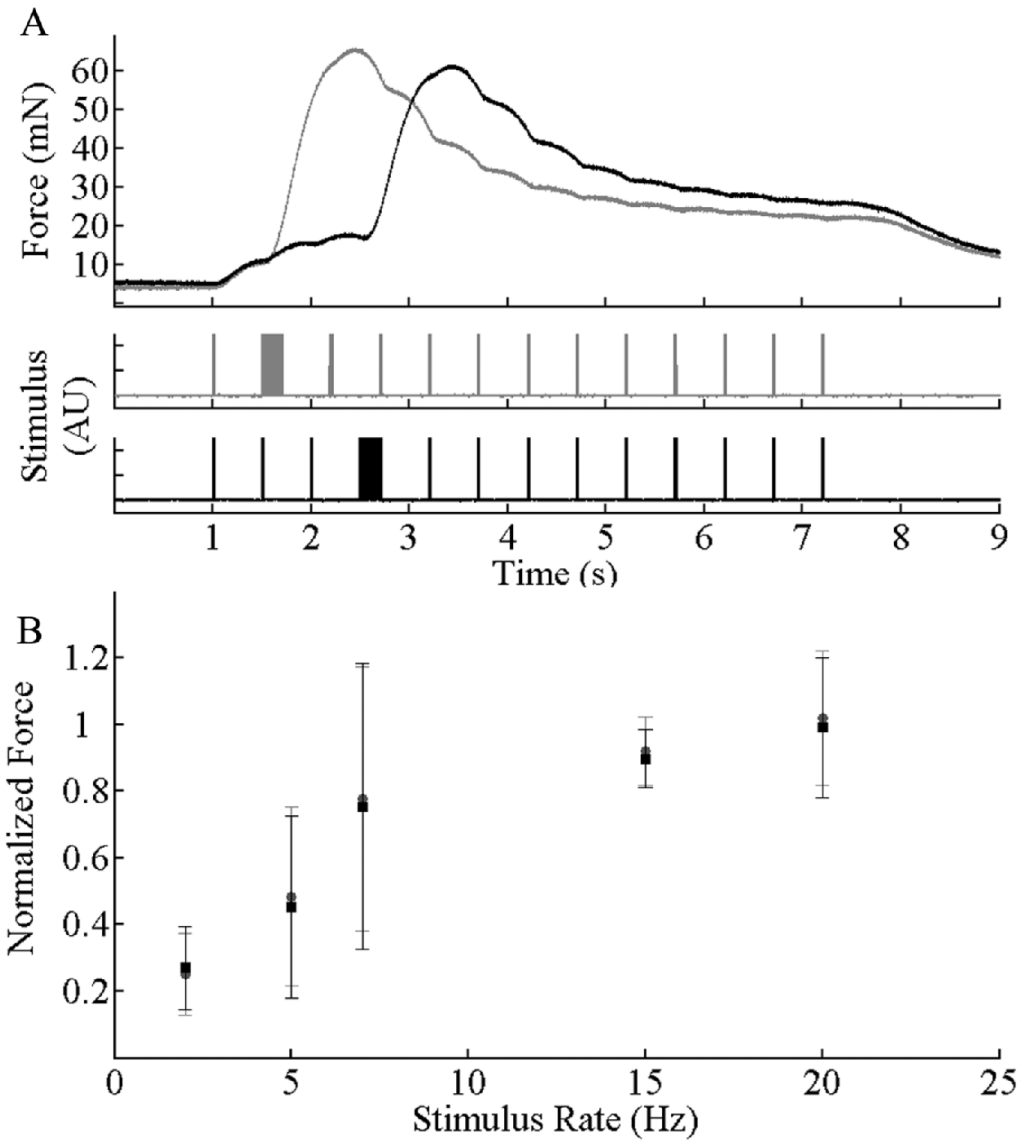

Figure 12: **Force generation with varying onsets of a hysteretic burst**. (A) Each trace is the average of 5 repetitions in a single animal. Data from a tetanic stimulus train with a hysteretic burst at t = 1.5 s are shown in gray, whereas data recorded from a tetanic train with a hysteretic burst at t = 2.5 s are shown in black (stimulus trains are shown below). (B) Variations in onset plotted as a function of stimulus frequency. Differences are not statistically different (n = 9 animals). Data points are the mean of 15-25 trials of each rate, error bars = standard error of the mean.

Finally, a third stimulus paradigm was explored in which three high frequency bursts were inserted in an otherwise constant 12.5 s stimulus rate. As the longitudinal muscles are stimulated to contract, the position of the force transducer allowed for the isometric contraction of the muscles, as muscle length did not change. Such an experimental design limits the amount that actin and myosin can overlap, and would imply that even small changes in force steps suggests hysteretic forces are not dependent on the amount of overlap between actin and myosin. As a result, the force production during multiple bursts revealed that the overall increase in force recruited by each additional hysteretic burst was non-unitary (Figure 13A).

Force generation was measured as a change from baseline at four different times: (1) at t ~3.9, before the first high frequency burst, (2) at t ~6.9 s, after the first high frequency burst, (3) at t ~9.9 s, after the second high frequency burst, and (4) at t ~12.5 s, after the third and final high frequency burst (Figure 14A). Force generation continued to remain elevated after each high frequency burst (Figure 14B). The largest increase in force production occurred following the first high frequency burst at t ~4.0 s. Force generation increased by 147.4%, 32.8%, and 28.4% from F1 to F2, when stimulated at 2 Hz (♦), 5 Hz (■), and 15 Hz (●) respectively. Each subsequent high frequency burst resulted in a smaller increase in force (Figure 14C).

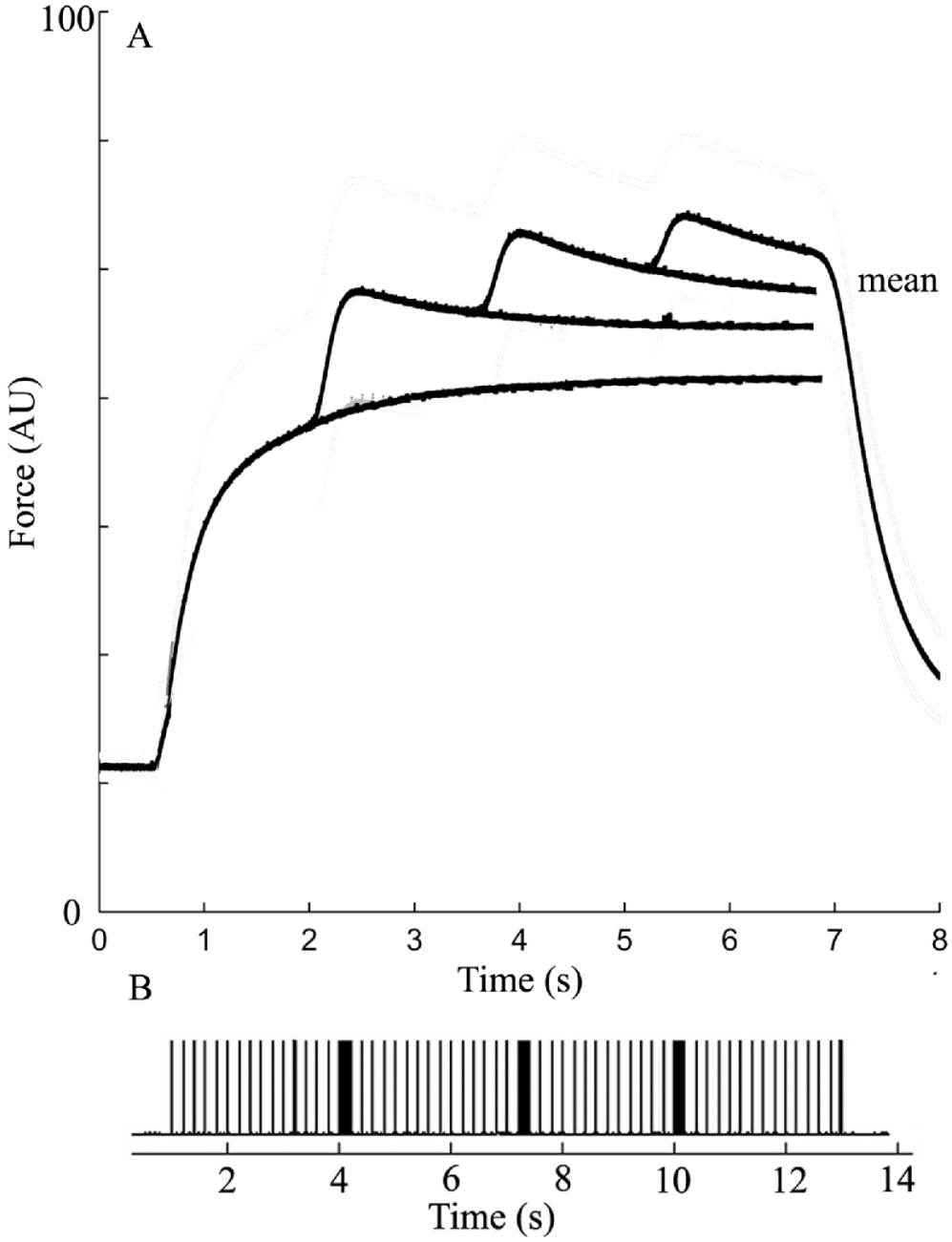

Figure 13: **Force generation upon stimulation with tetanic *and* multiple hysteretic bursts**. (A) Force trace is average of 10 trials, each from a single animal, using a 5 Hz constant stimulus train. Multiple bursts and the resulting forces were fit with logarithmic lines for visualization purposes only; in each trial, all three bursts were present (as shown in *B*). The extrapolated lines are shown to illustrate that increases in force recruitment by each additional hysteretic burst is non-unitary.

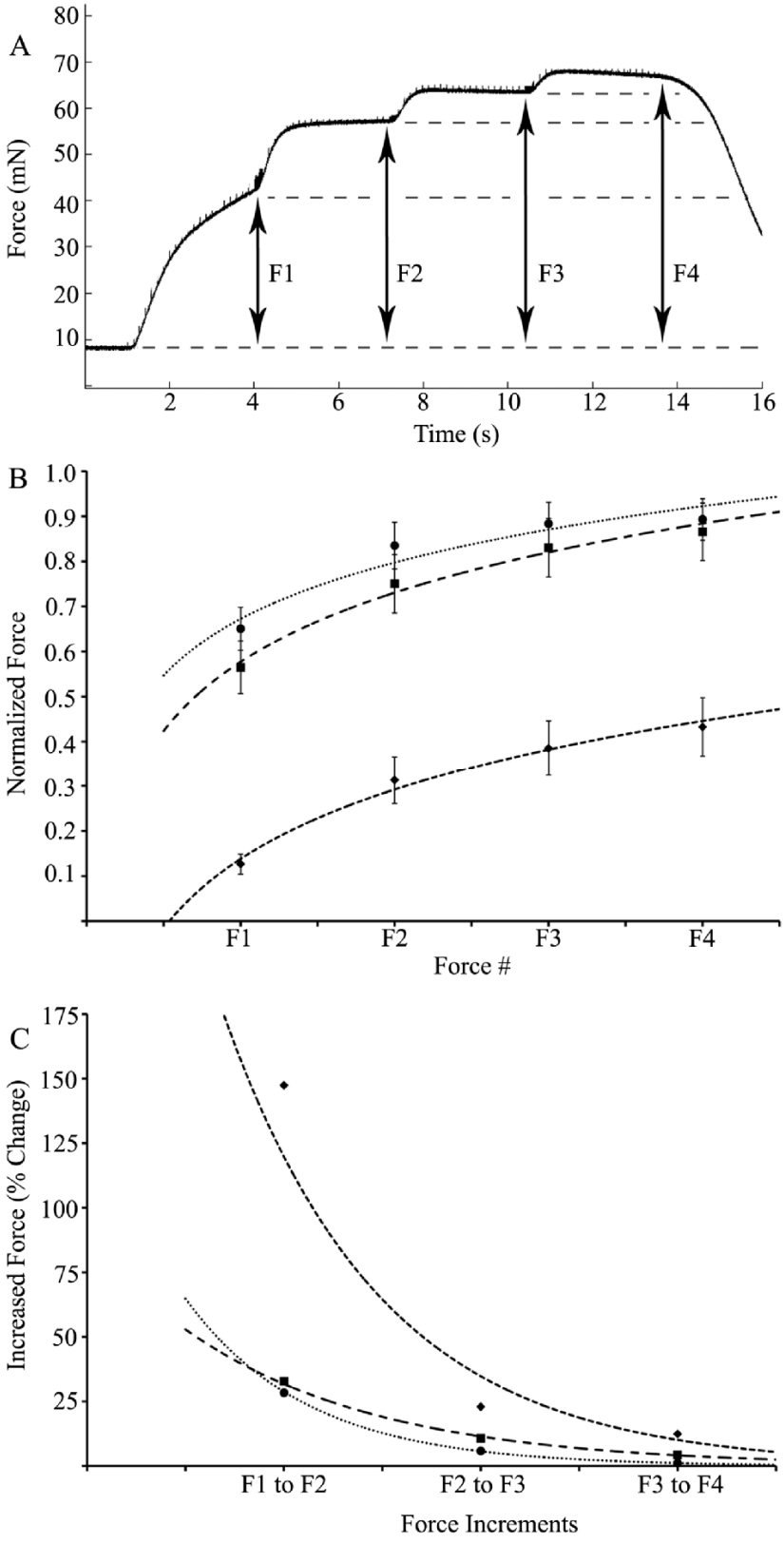
A
Force (mN)
80
70
60
50
40
30
20
10
F1
F2
F3
F4
2
4
6
8
10
12
14
16
Time (s)
B
Normalized Force
1.0
0.9
0.8
0.7
0.6
0.5
0.4
0.3
0.2
0.1
F1
F2
F3
F4
Force #
C
Increased Force (% Change)
175
150
125
100
75
50
25
F1 to F2
F2 to F3
F3 to F4
Force Increments

Figure 14: **Force generation after each subsequent multiple hysteretic burst.** (A) Force trace is the average of 10 trials, each from a single animal, using a 7 Hz constant stimulus train. Force generation was measured as change from baseline. (B) Maintained force generation measured after the occurrence of the high frequency burst. Each data point is mean force generation calculated from 20 trials using stimulus trains of 2 Hz (♦) and 5 Hz (■), and 40 trials using a stimulus train of 15 Hz (●). Total animals used (n) = 7 and errorbars = standard error of the mean. (C) The hysteretic burst generates smaller relative changes in peak force after earlier hysteretic bursts. Force generation appears to decrease exponentially with later occurrences of high frequency bursts. This is shown as percentage change in force generation from F1 to F2, F2 to F3, and F3 to F4.

DISCUSSION

Third instar *Sarcophaga* muscle cells have the capacity for hysteretic force production as synaptic facilitation does not occur during, or after, high frequency, hysteretic bursts. The largest changes in force production occurred over lower MN rates, with a high frequency burst occurring three seconds into the stimulus train. Statistically insignificant differences in force production were found when the high frequency burst occurred at t = 1.5 s and t = 2.5 s. The presence of multiple high frequency bursts also suggested a non-unity hysteretic effect. Overall, tetanic force production saturated between 20 Hz–40 Hz. EJP voltage also demonstrated a negative correlation with increasing MN rates, but there was no apparent synaptic depression. Thus hysteresis appears to be a property of the post synaptic cell, the muscle, and seems to be related to characteristics of the contractile proteins other than the actin and myosin overlap in the sarcomere.

Tetanic activation of motoneurons showed a logarithmic rate-force relationship which saturated around 20 Hz at 0.92 (±0.03) AU. The longitudinal muscles of the larvae run the entire length of the body and account for a large amount of their physical mass. With such large muscles, this saturation rate seemed surprisingly low. However, it may be that the slow peristaltic locomotion characteristic of third instar *Diptera* requires only low MN rates. Early studies with crustacean muscle utilized modulating frequencies from 10-100 Hz (Wilson and Larimer, 1968), a range across which force would change very little in larval

Sarcophaga muscle. Furthermore, the normal contractile operating frequency of a high-frequency flagellum abductor muscle of the crab is 10 Hz (Josephson and Stokes, 1994). A normal operating frequency of 10 Hz in fast muscle strongly suggests that 20 Hz – 40 Hz stimulus rates are extremely uncharacteristic of slow-muscle and may not be behaviorally relevant. A typical correlation between stride speed and MN frequency in larval *Diptera* reveals crawling speeds ranging from 0.07 to 1.0 cm/s at frequencies ranging from 0.6 to 2.8 Hz (Berrigan and Pepin, 1995). The link to observed behavioral rates may contextualize the result that hysteresis is most profound at low MN rates. Increasing muscle contraction by inserting a high frequency burst, when actin and myosin are already cycling at maximum speed, might not be expected to render noticeable differences in force. Similar findings in which the hysteretic loops decrease in size as the modulation frequencies increase have been reported in crustacean muscle (Wilson and Larimer, 1968) and the *triceps surae* muscle of cats (Partridge,1965).

Hysteresis across the lower frequency rates may be behaviorally relevant even with the assumption that MN rates of 20 Hz – 40 Hz exceed normal operating frequencies. There is a well known, and behaviorally relevant, hysteretic relationship between stimulus frequency and isometric force in crustacean muscle. Increased force resulting from a high stimulus frequency is partially retained when the stimulus frequency is subsequently reduced (Blaschko et al., 1931; Wilson and Larimer, 1968), thereby decreasing the organism's cost of maintaining a tightly clamped shell.

Diptera may also utilize hysteresis to increase the efficiency of their locomotion. Larval crawling is accomplished by repeated peristaltic wave-like strides and involves molecules mediating neuronal signaling (Song et al., 2007). Larvae use their muscles to maintain tonus in their hydrostatic skeletons (Berrigan and Lighton, 1993). Instead of a hard skeleton, *Diptera* larvae use fluid and tissue pressure to stiffen the body for muscles to do useful work (Trimmer and Issberner, 2007). Any change in pressure as a result of a weakened cuticle might create a bulbous protrusion and interfere with normal locomotion. Expansion in unwanted directions could alter the sensory inputs involved in the peripheral feedback responsible for correct crawling movements. Thus, the capacity to quickly generate greater than normal forces (or hysteresis) would allow the organism to counteract the protrusion, and return tonus to the hydrostatic skeleton. Friction generated within the organisms (i.e. by fluid movement during peristalsis) could also impose disproportionate costs during high frequency movement (Berrigan and Lighton, 1993), and would further support the need for the larvae to limit the duration of high frequency MN rates.

As mentioned before, synaptic facilitation and augmentation were alternative explanations for hysteresis, and would support the dogma that force and voltage are proportional (Abbot and Aubert, 1952). Such findings have also received recent support at the neuromuscular junction of crustaceans in which augmentation at the NMJ was reported to increase and strengthen the muscle's force production (Stein et al., 2006). Calcium ions play crucial signaling roles in

many forms of synaptic facilitation; as all phases of enhancement are, with a few exceptions, attributable to a presynaptic increase in the number of transmitter quanta released (Zucker, 1999). Thus increased calcium build-up in the NMJ can result in strengthened neurotransmission (Atwood et. al., 1997). However, I found hysteresis to occur in the absence of synaptic facilitation or depression because EJP amplitudes after hysteretic, high frequency bursts do not show facilitation (Figure 10A). These findings illustrate that in this system, force is not exclusively voltage dependent (Wilson and Larimer, 1968; Wilson et al., 1970) and may be an example of muscle plasticity.

In the absence of clear voltage dependence for force production, closer attention should be paid to molecular mechanisms of force generation in muscle fibers. The custom silicon strain gauge force transducer used in this work only tolerates nominal changes in length during contraction. Therefore, hysteresis in our experimental animals was occurring under isometric conditions. If the length does not change, then the extent to which myosin and actin does not change, suggesting that hysteretic forces are not dependent upon the amount of overlap between actin and myosin. This is consistent our failure to elicit hysteresis during the muscle shortening phase (Figure 12A) and with previous findings in which sarcomere length non-uniformity was not found to be a lone operative in the hysteretic phenomenon (Herzog and Leonard, 2002). The failure of the cross-bridge cycling theories to explain high speed lengthening in skeletal muscle (Harry et. al., 1990) is another example of hysteretic behavior that cannot be

solely dependent on the interaction of actin and myosin filaments. Thus, assuming the mechanism for hysteresis resides in the muscle cell, another likely mechanical source could be titin or kettin-like proteins. One exciting investigation to help elucidate the molecular underpinnings of hysteresis will be the analysis of hysteresis in mutants for contractile proteins. Specifically, hysteresis in the muscles of the many *Drosophila* lines with mutations in proteins localized at the sarcomere could be studied.

Titin has already been well accepted as a storage protein for elastic energy in muscle cells (Tshhovrebova and Trinick, 2002). However, during isometric contractions, titin is unable to stretch to full capacity, and hysteresis may result from a biochemical change to the protein or its surrounding elements. A topic of growing interest is the role of co-transmission in neural network modulation. Neuromodulatory substances, such as amines and neuropeptides, can influence the output of networks, and ultimately behavior (Nusbaum et al., 2001). Octopamine, a biogenic amine, is a major neuromodulator with neurotransmitter functions that mediates various physiological processes in the nervous systems of invertebrate species, including crustaceans, mollusks, and insects (Evans and Siegler, 1982). More specifically, octopamine has been shown to affect synaptic plasticity at glutamatergic neuromuscular synapses (Nishikawa and Kidokoro, 1999). In *Diptera,* L-glutatmate is a major neurotransmitter at the NMJ and is present at all motor nerve endings (Kawagoe et al., 1981). In catch tension in locust skeletal muscle, the identified octopaminergic neuron (DUMETi) is

suggested to change the response of muscle from one that favors maintenance of posture, to one that favors rapid changes in position or force – such as might occur during locomotion (Evans and Siegler, 1982).

In the previously described study, the application of octopamine to the locust skeletal muscle greatly reduces the amount of catch tension displayed. However, there have been comparisons made between the octopaminergic/tyraminergic and the vertebrate adrenergic system. This includes the illustrious role of the adrenergic/octopaminergic signaling, the fight or flight response. The fight or flight response is synonymous for the quick adaptation to energy-demanding situations and stressful stimuli. It would induce the metabolic and behavioral adaptations leading to enhanced energy supply, increased muscle performance, and matched behaviors (Roeder, 2005) – similar to hysteresis.

Finally, a more familiar biochemical candidate for the hysteretic effect is Ca++. Muscle contraction is activated through the binding of calcium ions to Ca++-sensitive myofibrillar or sarcoplasmic proteins (Ridgway et al., 1983). In all muscle types, the binding of Ca++ allows actin and myosin to interact. Although we could not see a visible intracellular presynaptic change in voltage, one possible hypothesis is a shift in Ca++ sensitivity when relaxing, resulting in a hysteretic force production between varying concentrations of free Ca++ (Ridgway et al., 1983). One simple explanation is that a change in force leads to a change in Ca++ binding, with a possible mechanism involving a change in calcium affinity for binding sites on the myofilaments. The feedback from force

to Ca++ sensitivity in the post-synaptic cell may also contribute to the hysteretic effect.

The role of Ca++ in synaptic transmission may also account for the apparent decrease in EJP amplitude with increasing stimulus frequencies. High frequency stimulus trains maximize the release of C++ thereby raising the membrane potential and maximum peak voltage (Figure 11D). The decrease in EJP amplitude may result from depolarization due to the saturation of Ca++ and other cations, with the high frequency stimulus preventing the return of the membrane potential to baseline levels.

In addition to reports of hysteresis in arthropod muscle, several investigators have reported a similar phenomenon in skeletal muscle (Partridge, 1965; Peterson et al., 2004; Herzog and Rassier, 2006). The occurrence of the hysteretic phenomenon across numerous animal species – including mammalian, insect, crustacean, frog, and shark muscle (Wilson et. al., 1970) – suggests further characterization is critical to understanding its role in force transduction and its transformation in the post synaptic muscle. Working with *Sarcophaga bullata*, provides a simple system in which a quantitative evaluation of the different components of the transduction phenomenon can be broken down. As of yet, no broad comparative work has assimilated the many observations across diverse phylogeny. However, the occurrence of hysteretic like incidences throughout varies species, suggests that hysteresis may be a general mechanism of muscle and should be accounted for in models of muscle function and contraction. And

while the hysteretic mechanism still remains poorly understood, research involving *Diptera*, may offer a solid platform to begin broader comparative work. A thorough understanding of hysteresis (in *Diptera*), may help elucidate the impact hysteresis has on behavior and general strategies of neuromuscular control.

LITERATURE CITED

Abbott, B.C. and Aubert, X.M. 1952. The force exerted by active striated muscle during and after change of length. J. Physiol. 117: 77-86.

Atwood, H.L. 1967. Crustacean neuromuscular mechanisms. Amer. Zool. 7: 527-551.

Atwood, H.L., Hoyle, G., and Smyth Jr., T. 1965. Mechanical and electrical responses of single innervated crab-muscle fibers. J. Physiol. 180: 449-482.

Atwood, H.L., Karunanithi, S., Georgiou,J., and Charlton, M.P. 1997. Strength of synaptic transmission at a neuromuscular junctions of crustaceans and insects in relation to calcium entry. Invert. Neurosci. 3:81-87

Bennet-Clark, H.C. 1977. Storage of elastic strain energy in muscle and other tissues. Nature 265: 114-117.

Berchold, M.W., Heinrich, H., and Muntener, M. 2000. Calcium ion in skeletal muscle: Its crucial role for muscle function, plasticity, and disease. Physiol Rev 80: 1215-1265.

Berrigan, D. and Lighton, J.R.B. 1993. Bioenergetic and kinemtic consequences of limblessness in larval *Diptera*. J. Exp. Biol. 179: 245-259.

Berrigan, D. and Pepin, D. 1994. How Maggots Move: Allometry and Kinematics of Crawling in Larval *Diptera*. J. Physiol. 41: 329-337.

Blaschko, H., Cattell, M., and Kahn, J.L. 1931. On the nature of the two types of response in the neuromuscular system of the crustacean claw. J. Physiol. 73: 25-35.

Bullard, B., Garcia, T., Benes, V., Leaker, M., Linke, W.A., and Oberhauser, A.F. 2006. The molecular elasticity of the insect flight muscle proteins projectin and kettin. Proc. Nat. Acad. Sci. 103: 4451-4456.

Evans, P.D and Siegler, M.V.S. 1982. Octopamine mediated relaxation of maintained and catch locust skeletal muscle. J. Physiol. 93-112.

Gojdosik, R.L. 2001. Passive extensibility of skeletal muscle: review of the literature with clinical implications. Clin. Biomech. 16: 87-101.

Harry, J.D., Ward, A.W., Heglund, N.C., Morgan, D.L., and McMahon, T.A. 1990. Cross-bridge cycling theories cannot explain high-speed lengthening behavior in frog muscle. Biophys J. 57: 201-208.

Harrison, S.M., Lamont, C., and Miller, D.J. 2008. Hysteresis and the length dependence of calcium sensitive in chemically skinned rat cardiac muscle. J. Physiol.401: 115-143

Herzog, W. and Leonard, T.R. 2002. Force enhancement following stretching of skeletal muscle: a new mechanism. J. exp. Biol. 205: 1275-1283.

Hill, A.V. 1952. The mechanics of active muscle. Proc. Roy. Soc. Lond. B, Biol. Sci. 141: 104-117.

Hooper, S.L. and Thuma, J.B. 2004. Invertebrate muscles: Muscle specific genes and proteins. Physiol Rev 85: 1001-1060.

Huxley, A.F. 2000. Mechanic and models of the myosin motor. Phil. Trans. R. Soc. Lond. B 355: 433-440

Josephson, R.K. and Stokes, D.R. 1989. Strain, muscle length and work output in a crab muscle. J. Exp. Biol.145: 45-61

Josephson, R.K. and Stokes, D.R. 1994. Contractile properties of a high-frequency muscle from a crustacean. J. Exp. Biol. 187: 295-303.

Kawagoe, R., Onodera, K. and Takeuchi, A. 1981. Release of glutamate from the crayfish neuromuscular junction. J. Physiol 312: 225-236.

Lappin, A.K., Monroy, J.A., Pilarski, J.Q., Zepnewski, E.D., Pierotti, D.J., and Nishikawa, K.C. 2006. Storage and recovery of elastic potential energy powers ballistic prey capture in toads. J. Exp. Biol. 209: 2535-2553.

Nishikawa, K. and Kidokoro, Y. 1999. Octopamine inhibits synaptic transmission at the larval neuromuscular junction in *Drosophila melanogaster*. Brian Research 837: 67-74.

Nusbaum, M.P, Blitz,D.M., Swensen, M.A., Wood, D., and Marder, E. 2001. The roles of co-transmission in neural network modulation. Trnds. Neurosci. 24:146-154.

Partridge, L.D. 1965. Modifications of neural output signals by muscles: a frequency response study. J. Appl Physiol. 20: 150-156.

Partridge, L.D. 1966. Signal-handling characteristics of load-moving skeletal muscle. Amer. J. Physiol. 210: 1178-1191.

Purves, D, Augustine, G.J., Fitzpatrick, D., Hall, W.C., LaMantia, A., McNamara, J.O., and Williams, S.M., eds. 2004. *Neuroscience*, 3e, Sinauer Associates, Inc., Sunderland.

Ridgway, E.B., Gordon, M.A., and Martyn, A.D. 1983. Hysteresis in the force-calcium relation in muscle. Science 219: 1075-1077.

Roeder, T. 2005. Tyramine and octopamine: ruling behavior and metabolism. Annu. Rev. Entomol. 50: 447-77.

Sherwood, L. 2007. *Human physiology: From cells to systems*, 6e, Thomson Brooks/Cole, Belmont.

Song, J. and Kiureghian. 2006. Generalized Bouc-Wen model for highly asymmetric hysteresis. J. Engin. Mech.-ASCE 132: 610-618.

Song, W., Onishi,M., nuktidentric Jan, L.Y., and Jan, Y.N. 2007. Peripheral multidentric sensory neurons are necessary for rhythmic locomotion behavior in *Drosophila* larvae. Proc. Nat. Acad. Sci. 104: 5199-5204.

Spudich, J.A. 2001. The myosin swinging cross-bridge model. Nature Rev. 2: 387-391.

Stein, W., Smarandache, C.R. Nickmann, M., and Hedrich, U.B.S. 2006. Functional consequences of activity-dependent synaptic enhancement at a crustacean neuromuscular junction. J. Exp. Biol. 209: 1285-1300

Strausfeld, N. and Singh, H. 1983. Lucifer yellow histology. In N. Strausfeld (Ed.), Functional Neuroanatomy, Springer, Berlin. pp.132-155.

Trimmer, B. and Issenberner, J. 2007. Kinematics of soft-bodied, legged locomotion in *Manduca sextra* larvae. Biol. Bull. 212: 130-142.

Tsihhovrebova, L. and Trinick, J. 2002. Role of titin in vertebrate striated muscle. Phil. Trans. R. Soc. Lond. B 357: 199-206.

Usherwood, P.N.R. and Machili, P. 1968. Pharmacological properties of excitatory neuromuscular synapses in the locust. J. Exp. Biol. 49: 341-361

Wilson, D. M. and Larimer, J. L. 1968. The catch property of ordinary muscle. Proc. Nat. Acad. Sci. 61: 909-916

Wilson, D.M., Smith, D.O., and Dempster, P. 1970. Length and tension hysteresis during sinusoidal and step function stimulation of arthropod muscle. Amer. J. Physiol. 218: 916-922.

Zucker, R.S. 1999. Calcium- and-activity-dependent synaptic plasticity. Crnt. Opin. in Neurobio. 9: 305-313.

Zucker, R.S. and Regehr, W.G. 2002. Short-term synaptic plasticity. Annu. Rev. Physiol. 64: 355-405.